Proceedings of CHT-17
ICHMT International Symposium on Advances in Computational Heat Transfer

May 28-June 1, 2017, Napoli, Italy

CHT-17-075

HEAT TRANSFER CHARACTERISTICS OF AN ELECTROOSMOTIC FLOW OF VISCOELASTIC FLUID IN SLIT MICROCHANNEL

Prakash Goswami[1§], Suman Chakraborty[2]
[1]Indian Institute of Petroleum & Energy, Visakhapatna, Andhra Pradesh-530003, India.
[2]Department of Mechanical Engineering, Indian Institute of Technology Kharagpur, West Bengal-721302, India
[§]Correspondence author. Email: ami.prakash@gmail.com

ABSTRACT In this work, we derive an analytical solution for heat transfer characteristics of a thermally developing flow of viscoelastic fluids under the application of an electroosmotic force. The walls are subjected to either in isothermal condition or a constant wall heat flux is employed. First, we derive a Helmholtz-Smoluchowski (HS) type slip velocity for the viscoelastic fluids, which is further used to simplify the energy equation. The Laplace transform method is employed with respect to the longitudinal variable to get a reduced form of the energy equation. The resulting expressions are inverted using residue calculus and as well as a Fourier series based numerical method to obtain the temperature distribution within the microchannel. Based on the analytical solution, we also derive an expression for the local heat transfer coefficient and Nusselt number. Two types of viscoelastic fluids, linear and exponential PTT fluid, are considered here. From this study it is found that, with increasing viscoelastic parameter, the advective heat transport is more in case of exponential-PTT fluid compared to linear-PTT fluid and hence requires less channel entrance length to reach at the fully developed state. The results obtained here, may have important implication towards the thermal management of bio-microfluidic devices.

Nomenclature

De	Deborah number	ε	Permittivity of the medium (F/m)
e	Elementary charge (C)	ψ	EDL potential (V)
E_x	Applied electric field (V/m)	ζ	Zeta potential (V)
J	Non-dimensional Joule heat	κ^{-1}	EDL thickness (m)
k_B	Boltzmann constant (J/K)	ξ	Non-dimensional channel length
k_f	Thermal conductivity (W/mK)	η	Non-dimensional channel height
$n^{\pm}$	Cationic/anionic number densities (m^{-3})	$\boldsymbol{\tau}$	Viscoelastic stress tensor
n_0	Bulk ionic number density(m^{-3})	μ	Fluid viscosity (kg/ms)
Nu_ξ	Local Nusselt number	λ	Relaxation time of the fluid
Pe_T	Thermal Peclet' number	σ	Extensibility parameter of the fluid
q''_W	Wall heat flux (W/m^2)	σ_b	Bulk ionic conductivity (S/m)
Q''_W	Non-dimensional wall heat flux	ρ_f	Fluid density (kg/m^3)
T	Absolute temperature (K)	c_P	Specific heat capacity (J/kg K)
T_0	Inlet temperature (K)	Θ	Non-dimensional temperature

T_W	Wall temperature (K)	Θ_m	Non-dimensional mean temperature
U_{HS}	Helmholtz-Smoluchowski velocity (m/s)	$tr\boldsymbol{\tau}$	Trace of stress tensor $\boldsymbol{\tau}$
z	Valence	*Erfi*	Imaginary error function

INTRODUCTION

The advent of miniaturization made enormous progress through the novel electroosmotic flow (EOF) actuation mechanism, where an ionic solution is driven by an externally applied electric field within a charged narrow confinement (Hunter [1981], Probstein [1994]). To maintain a high throughput, the conventional pressure pumps are more prone to mechanical failure, whereas the electroosmotic pump does not require such mechanical parts and can transport the fluid by exploiting the fluid-solid interfacial characteristics together with an external electric field. The simplicity of the device leads to the development of a huge proportion of the microfluidic devices, such as bio-micro/nanofluidic devices, cooling of MEMS, muTAS, Lab-on-a-Chip, etc. A common feature of EOF is the plug-like velocity profile which reduces the dispersion of transported samples. On the other hand, the high electric field strength and conductivity of the solution lead to the Joule heat which may have adverse effect on the transport of thermally labile biological samples. Therefore, besides the volumetric transport the thermal management of the device also become important for design optimality.

The suitability of EOF in thermal management of microelectronic devices was also explored (Maynes and Webb [2003a-b, 2004], Horiuchi and Dutta [2004], Tang et al. [2004], Dutta et al. [2006], Das and Chakraborty[2006], Chen [2009], Dey et al. [2011, 2013], Xuan and co-workers[2004a-b, 2005, 2008]) extensively. Maynes and Webb [2003a-b, 2004] have thoroughly discussed the thermal characteristics of an electroosmotic flow. They analytically investigated the thermally fully developed electroosmotic flow in a parallel plate and circular microchannel, neglecting the viscous dissipation. They have shown that the Nusselt number in case of a thermally developed flow reaches to 12 for parallel plate channel and 8 for circular channel (based on the hydraulic diameter of the channel). The effect of viscous dissipation becomes important for higher electrical double layer thickness. This has been further extended to thermally developing flows by Boderick et al. [2005] and Iverson et al. [2004]. In another study, Horiuchi and Dutta [2004] have described the thermally developing EOF for thin electric double layer and small zeta potential. They have analytically obtained an expression for the local Nusselt number and the temperature distribution by considering an isothermal wall and constant heat flux at the microchannel walls. In microchannels the main factors for heat transfer appeared to be the viscous dissipation and Joule heating. In case of an electroosmotic flow with weaker electrical double layer, the Joule heat becomes significant compared to the viscous dissipation as Joule heating occurs over the entire volume whereas the viscous dissipation is entirely restricted within the electrical double layer which is a small region adjacent to surface (Horiuchi and Dutta [2004]). This simplified analysis have been used extensively for theoretical studies in microchannel heat transfer.

Although initially these studies were restricted to the Newtonian fluids, but the importance of microfluidics in the field of biosciences opens up a new regime which is EOF of non-Newtonian fluids and have drawn much attention in recent times (Zhao and Yang [2013]). Most commonly, the biofluids that are used for analysis and detection schemes are blood or DNA solutions, which shows viscoelastic behavior and have different flow characteristics than that of Newtonian fluids (Park and Lee [2008a,b]). In addition to this, particular interest was also shown towards the thermal characteristics of electroosmotic flow of non-Newtonian fluids (Sadeghi et al. [2010, 2011], Escandon et al. [2011, 2013], Sanchez et al. [2013], Yavari et al. [2013], Goswami et al. [2016]). Sadeghi et al. [2011] have studied the heat transfer due to a fully developed electroosmotic flow of Phan-Thien-Tanner (PTT) and FENE-P viscoelastic fluids under the Debye-Huckel linearization

and shown that the viscous dissipation effect is important for low values of viscoelastic parameter and Debye layer thickness. Escandon et al. [2011] studied the conjugate heat transfer in a microchannel considering the flow of PTT fluid under the combined influence of electroosmotic and pressure forces. As a follow up, a lubrication theory based thermal analysis of PTT fluids are performed by Bautista et al. [2013] considering temperature dependent viscosity, viscoelastic relaxation parameter and liquid conductivity. Coelho et al. [2012] obtained an analytical expression for heat transfer in fully developed channel flow of simplified Phan-Thien-Tanner fluid with constant physical properties under electroosmotic and pressure forces. As far as our concern, in theoretical frameworks the heat transfer characteristics for viscoelastic fluids are mostly carried out for thermally fully developed flow and very little interest were shown towards thermally developing flows. Therefore, in this study we will focus on the thermally developing flow of viscoelastic fluids under electroosmotic forces.

In this study, we investigate the temperature distribution, heat transfer coefficient and the Nusselt number for a steady electroosmotic flow of viscoelastic fluid in a slit microchannel. Considering a thin electrical double layer adjacent to the surface, an analytical expression for the velocity profile is obtained for a viscoelastic fluid, which is further approximated by a Helmholtz-Smoluchowski (HS) type slip velocity close to the wall. In thermal analysis, the walls are assumed to be isothermal or maintain a constant heat flux. In the energy equation, the effect of Joule heat is considered explicitly together with the advective and diffusive terms. Since we are confined our study within the thin EDL regime, the effect of viscous dissipation is neglected. A simplified model for energy equation based on the HS slip velocity is solved to quantify the heat transfer characteristics for a thermally developing flow of viscoelastic fluid.

THEORETICAL FORMULATION

Electric Potential distribution Consider the electroosmotic flow of a viscoelastic fluid in a parallel plate microchannel having height 2H and length L, where L>>H (as depicted in Figure 1). The fluid is

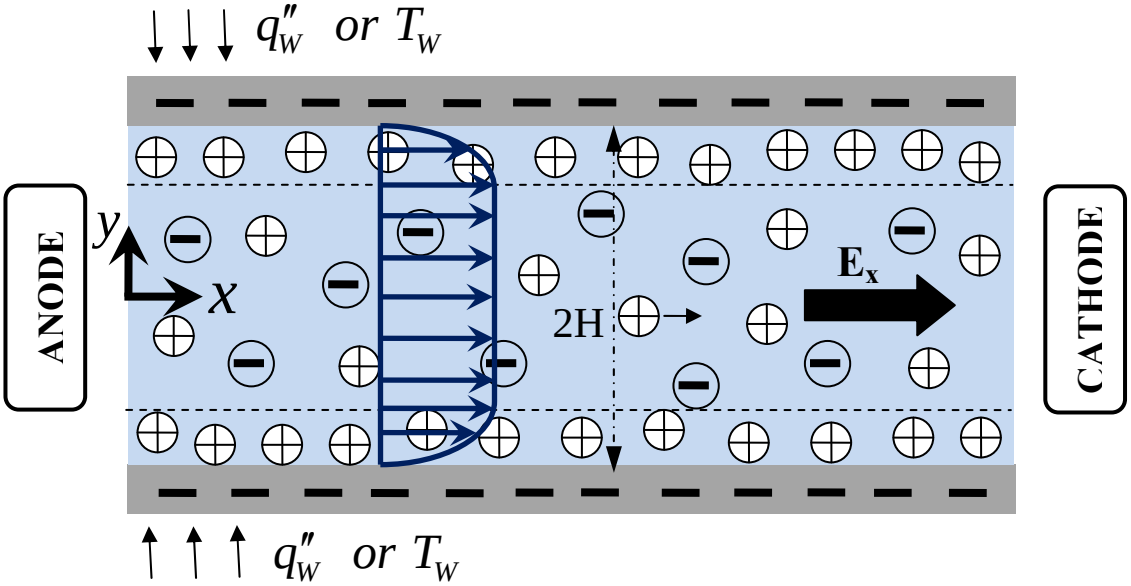

Figure 1: Schematic of the problem considered. The microchannel walls are isothermal or subjected to constant heat flux.

presumably an electrolyte solution having constant density and permittivity. The surfaces of the microchannel exhibit ionic properties in presence of the fluid and creates an electrical double layer (EDL) adjacent to the surface. When an electric field is applied, the ionic imbalance within the EDL

produces a strong electromotive force which results in an overall dragging of the fluid along the channel. This dragging of liquid is referred as the electroosmotic flow. For simplicity, we consider a symmetric (z:z) electrolyte. The co-ion and counter-ion number densities $n^{\pm}$ are given by the Boltzmann distribution $n^{\pm} = n_0 Exp\left[\mp ez\psi / k_B T\right]$, where, n_0 represents the bulk concentration of the ions, ψ represents the EDL potential, e is the elementary charge, z is the valence of the ions, k_B is the Boltzmann constant, and T is the absolute temperature. The total ionic charge density is given by $\rho_e = ez\left(n^+ - n^-\right)$ which is related to the EDL potential distribution ψ by the Poisson equation $\varepsilon\nabla^2\psi = -\rho_e$, where ε is the permittivity of the medium. The potential at the surface of the microchannel is often characterized by a zeta potential ζ. For $\zeta \ll k_B T / ez$, a Debye-Hückel approximation can be employed to obtain a simplified form of the Poisson equation, which reads

$$\nabla^2\psi = \kappa^2\psi \tag{1}$$

where κ^{-1} represent the characteristic EDL thickness and is given by $\kappa^2 = (2n_0 e^2 z^2)/(\varepsilon k_B T)$. In the present configuration, the solution of the above equation (1) can be obtained by employing a symmetry condition at the channel central line, i.e., $d\psi/dy = 0$ at $y = 0$ and a specified zeta potential at the wall, i.e., $\psi = \zeta$ at $y = H$. The solution of (1) is given by

$$\psi = \zeta \cosh(\kappa y)/\cosh(\kappa H) \tag{2}$$

Equation (2) provides the potential distribution within the microchannel under thin EDL approximation.

Velocity profile An externally applied electric field, E_x, in the channel x-direction causes an electroosmotic body force $\rho_e E_x$, which drives the electrolyte solution in the direction of the electric field. The dynamics of the fluid is governed by the mass conservation and the Cauchy equation of motion

$$\begin{aligned} \nabla\bullet\mathbf{u} &= 0 \\ 0 &= \nabla\bullet\boldsymbol{\tau} + \rho_e E_x \end{aligned} \tag{3}$$

where $\boldsymbol{\tau}$ represents the viscoelastic stress tensor for a simplified Phan-Thien-Tanner fluid. In case of a steady fully developed flow the stress components are given by

$$\begin{aligned} f\left(tr\boldsymbol{\tau}\right)\tau_{xx} &= 2\lambda\frac{\partial u}{\partial y}\tau_{xy} \\ f\left(tr\boldsymbol{\tau}\right)\tau_{yy} &= 0 \\ f\left(tr\boldsymbol{\tau}\right)\tau_{xy} &= \mu\frac{\partial u}{\partial y} + \lambda\frac{\partial u}{\partial y}\tau_{yy} \end{aligned} \tag{4}$$

From (3) and (4), with the condition $\tau_{xy} = 0$ at $y = 0$, one can readily obtain

$$\frac{du}{dy} = \frac{1}{\mu} f\left(\tau_{xx}\right)\varepsilon E_x \frac{d\psi}{dy} \tag{5}$$

where $\tau_{xx} = \frac{2\lambda}{\mu}\left(\varepsilon E_x \frac{d\psi}{dy}\right)^2$. Integrating equation (5) and using the no-slip boundary condition $u = 0$ at $y = H$, gives the velocity profile as

$$u(y) = -\frac{\varepsilon E_x}{\mu}\int_y^H f\left(\tau_{xx}\right)\frac{d\psi}{dy}dy \tag{6}$$

In this analysis, we consider the cases of a linear-PTT (LPTT) model and an exponential-PTT (EXPTT) model for the fluid. Accordingly, the function $f\left(\tau_{xx}\right)$ can be given in the form

$$\begin{aligned} f\left(\tau_{xx}\right) &= 1+\frac{\sigma\lambda}{\mu}\tau_{xx} \qquad ; Linear\ PTT \\ &= Exp\left[\frac{\sigma\lambda}{\mu}\tau_{xx}\right]; Exponential\ PTT \end{aligned} \tag{7}$$

where μ is the fluid viscosity, λ is the relaxation parameter and σ is the extensibility parameter. Using (7), from (6), the velocity profiles are obtained as

$$\begin{aligned} u^{LPTT}(y) &= -\frac{\varepsilon\zeta E_x}{\mu}\left\{\left(1+\frac{3}{2}\frac{\sigma De^2}{\cosh^2(\kappa H)}\right)\left(1-\frac{\cosh(\kappa y)}{\cosh(\kappa H)}\right)+\frac{\sigma De^2}{6}\frac{\cosh(3\kappa H)}{\cosh^3(\kappa H)}\left(1-\frac{\cosh(3\kappa y)}{\cosh(3\kappa H)}\right)\right\} \\ u^{EXPTT}(y) &= -\frac{\varepsilon\zeta E_x}{\mu}\left\{\frac{Exp(-B)}{\sqrt{B}\cosh(\kappa H)}\frac{\sqrt{\pi}}{2}Erfi\left(\sqrt{B}\cosh(\kappa H)\right)\left(1-\frac{Erfi\left(\sqrt{B}\cosh(\kappa y)\right)}{Erfi\left(\sqrt{B}\cosh(\kappa H)\right)}\right)\right\} \end{aligned} \tag{8}$$

where the Deborah number $De = \lambda\left(-\frac{\varepsilon\zeta E_x}{\mu}\right)\kappa$ and $B = \frac{2\sigma De^2}{\cosh^2(\kappa H)}$.

To obtain a Helmholtz-Smoluchowski type slip velocity for the above flows, we consider that the wall is located at $Y = 0$ and far from the wall the velocity reaches a maximum uniform value U_{HS}^{LPTT} (U_{HS}^{EXPTT}) for a linear-PTT (exponential-PTT) fluid . In typical microchannel flows the EDL potential ψ decreases exponentially from ζ to 0 over the distance κ^{-1} from the wall. Since, κ^{-1} is much smaller than the channel dimension, κY represents a relative value for the EDL thickness. A large value of κY represents a thinner EDL and the vice versa. Therefore, the EDL potential ψ can be approximated as $\psi \approx \zeta Exp[-\kappa Y]$. Using this potential distribution in (6) together with the boundary conditions $du/dy \to 0$ as $\kappa Y \to \infty$ and $u = 0$ at $\kappa Y = 0$ gives the velocity profiles as

$$\begin{aligned} u^{LPTT}(Y) &= -\frac{\varepsilon\zeta E_x}{\mu}\left\{\left(1-e^{-\kappa Y}\right)+\frac{2}{3}\sigma De^2\left(1-e^{-3\kappa Y}\right)\right\} \\ u^{EXPTT}(Y) &= -\frac{\varepsilon\zeta E_x}{\mu}\left\{\frac{Erfi\left(\sqrt{2\sigma De^2}\right)}{\sqrt{2\sigma De^2}}\frac{\sqrt{\pi}}{2}\left(1-\frac{Erfi\left(\sqrt{2\sigma De^2}e^{-\kappa Y}\right)}{Erfi\left(\sqrt{2\sigma De^2}\right)}\right)\right\} \end{aligned} \tag{9}$$

Now employing the condition $u = U_{HS}^{LPTT}$ or U_{HS}^{EXPTT} as $\kappa Y \to \infty$ gives the slip velocities of the form

$$\begin{aligned} U_{HS}^{LPTT} &= -\frac{\varepsilon\zeta E_x}{\mu}\left(1+\frac{2}{3}\sigma De^2\right) \\ U_{HS}^{EXPTT} &= -\frac{\varepsilon\zeta E_x}{\mu}\frac{\sqrt{\pi}}{2}\frac{Erfi\left(\sqrt{2\sigma De^2}\right)}{\sqrt{2\sigma De^2}} \end{aligned} \tag{10}$$

In equation (10), as $\sigma De^2 \to 0$ both are reduces to the Helmholtz-Smoluchowski slip velocity for a Newtonian case.

Temperature profile For a steady electroosmotic flow, the temperature distribution $T(x,y)$ within the fluid medium is governed by the equation

$$\rho_f c_P u(y)\frac{\partial T}{\partial x} = k_f\left(\frac{\partial^2 T}{\partial x^2}+\frac{\partial^2 T}{\partial y^2}\right)+\tau_{xy}\frac{du}{dy}+\sigma_b E_x^2 \tag{11}$$

where ρ_f is the fluid density, c_P is the specific heat capacity, k_f is the thermal conductivity, σ_b is the electrical conductivity of the bulk fluid. The term $\tau_{xy}\dfrac{du}{dy}$ and $\sigma_b E_x^2$ represents the volumetric heat generation due to viscous dissipation and Joule heating, respectively. As the velocity and potential gradient are mostly occurred within the EDL region, the variation of the viscous dissipation term is bounded within the EDL, whereas the Joule heating occurs throughout the channel. The viscous dissipation term has an order of magnitude $\sim \varepsilon^2\zeta^2 E_x^2/\mu H^2$ and Joule heating is in the order of $\sim \sigma_b E_x^2$. In typical electroosmotic flows the parametric values considered are: $\varepsilon \approx 10^{-10}\mathrm{C^2\times J^{-1}\times m^{-1}}$, $\zeta \approx 10-25\mathrm{mV}$, $\mu \approx 10^{-3}\mathrm{N\times s\times m^{-2}}$, $H \approx 10^{-4}-10^{-6}\mathrm{m}$ and $\sigma_b \approx 10^{-3}\mathrm{S\times m^{-1}}$. For a given electric field E_x, an order analysis shows that, the Joule heating term is much larger than the viscous dissipation term and may be dropped from equation (11) (Horiuchi and Dutta [2004]). Further neglecting the near wall velocity gradient and approximating the velocity by a uniform profile $U_{HS}\chi$, equation (11) can be written in the simplified form

$$\rho_f c_P U_{HS}\chi\frac{\partial T}{\partial x} = k_f\left(\frac{\partial^2 T}{\partial x^2}+\frac{\partial^2 T}{\partial y^2}\right)+\sigma_b E_x^2 \tag{12}$$

where $U_{HS}=-\dfrac{\varepsilon\zeta E_x}{\mu}$ and χ is $\left(1+\dfrac{2}{3}\sigma De^2\right)$ or $\dfrac{\sqrt{\pi}}{2}\dfrac{Erfi\left(\sqrt{2\sigma De^2}\right)}{\sqrt{2\sigma De^2}}$, according to LPTT or EXPTT fluid. To solve equation (12), the boundary conditions considered here are

$$\begin{aligned}
&T(x=0,y)=T_0\\
&T(x\to\infty,y)<\infty\\
&\partial T/\partial y=0 \quad at \quad y=0,\forall x\\
&T(x,y=H)=T_W \quad (\text{Isothermal wall condition})\\
&-k_f\partial T/\partial y=q_W'' \quad at \quad y=H \ (\text{Constant wall flux})
\end{aligned} \tag{13}$$

Here, T_0 is the inlet temperature, T_W is the temperature at the wall and q_W'' is the constant wall flux. Using the non-dimensional variables $\xi=x/H$, $\eta=y/H$, $\Theta=\left(T-T_0\right)/\left(T_W-T_0\right)$, equation (12) can be written in the form

$$Pe_T\chi\frac{\partial\Theta}{\partial\xi}=\left(\frac{\partial^2\Theta}{\partial\xi^2}+\frac{\partial^2\Theta}{\partial\eta^2}\right)+J \tag{14}$$

whereas the boundary conditions (13) takes the form

$$
\begin{aligned}
&\Theta(\xi=0,\eta)=0\\
&\Theta(\xi\to\infty,\eta)<\infty\\
&\partial\Theta/\partial\eta=0 \quad at\ \ \eta=0,\forall\xi\\
&\Theta(\xi,\eta=1)=1 \quad \text{(Isothermal wall condition)}\\
&\partial\Theta/\partial\eta=Q''_W \quad at\ \ \eta=1 \text{ (Constant wall flux)}
\end{aligned}
\tag{15}
$$

where $Pe_T=\rho_f c_P U_{HS} H/k_f$ is the thermal Peclet' number, $J=\sigma_b E_x^2 H^2/k_f\left(T_W-T_0\right)$ is the non-dimensional Joule heat and $Q''_W=-q''_W H/k_f\left(T_W-T_0\right)$ is the non-dimensional wall heat flux. To solve (14) with the boundary conditions (15), we employ the Laplace transform in ξ, which reduces the above equations in the form

$$
\begin{aligned}
&\frac{d^2\hat{\Theta}}{d\eta^2}-\alpha^2\hat{\Theta}=-\frac{J}{s}\\
&\frac{d\hat{\Theta}}{d\eta}=0 \qquad at\ \ \eta=0\\
&\hat{\Theta}=\frac{1}{s} \qquad at\ \ \eta=1 \text{ (Isothermal wall)}\\
&\frac{d\hat{\Theta}}{d\eta}=\frac{Q''_W}{s}\ at\ \ \eta=1 \text{ (Constant heat flux)}
\end{aligned}
\tag{16}
$$

where $\hat{\Theta}=\int_0^\infty e^{-s\xi}\Theta\left(\xi,\eta\right)d\xi$ and $\alpha^2=(Pe_T\chi-s)s$. Solving (16) one can get the temperature profile in the Laplace transform domain as

$$
\begin{aligned}
\hat{\Theta}&=\left(\frac{1}{s}-\frac{J}{\alpha^2 s}\right)\frac{\cosh\left(\alpha\eta\right)}{\cosh\left(\alpha\right)}+\frac{J}{\alpha^2 s};\ \text{for Isothermal wall}\\
&=\frac{Q''_W}{\alpha s}\frac{\cosh\left(\alpha\eta\right)}{\sinh\left(\alpha\right)}+\frac{J}{\alpha^2 s} \qquad ;\ \text{for constant heat flux}
\end{aligned}
\tag{17}
$$

Inverting (17) and using the residue calculus, the temperature profile for isothermal condition is obtained as

$$
\Theta\left(\xi,\eta\right)=1+\frac{J}{2}\left(1-\eta^2\right)+\sum_{n=0}^{\infty}\frac{2\lambda_n\left(-1\right)^n exp\left[\alpha_n\xi\right]}{\alpha_n\sqrt{Pe_T^2\chi^2+4\lambda_n^2}}\left(1+\frac{J}{\lambda_n^2}\right)\cos\left(\lambda_n\eta\right) \tag{18}
$$

where $\alpha_n=\frac{1}{2}\left(Pe_T\chi-\sqrt{Pe_T^2\chi^2+4\lambda_n^2}\right)$ and $\lambda_n=(2n+1)\pi/2$, whereas in case of constant wall heat flux the temperature distribution becomes

$$
\Theta\left(\xi,\eta\right)=\frac{\left(J+Q''_W\right)}{Pe_T^2\chi^2}\left(1+\xi Pe_T\chi\right)-Q''_W\left\{\left(\frac{1}{6}-\frac{\eta^2}{2}\right)-\sum_{n=1}^{\infty}\frac{2\left(-1\right)^n exp\left[\beta_n\xi\right]}{\beta_n\sqrt{Pe_T^2\chi^2+4\gamma_n^2}}\cos\left(\gamma_n\eta\right)\right\} \tag{19}
$$

where $\beta_n=\frac{1}{2}\left(Pe_T\chi-\sqrt{Pe_T^2\chi^2+4\gamma_n^2}\right)$ and $\gamma_n=n\pi$.

A numerical method based on the Fourier series approximation is also employed to invert equation (17) (Rice and Do [1995]). The analytical expressions obtained in equation (18) and (19) are matches

exactly with the numerical solution. Based on this analytical treatment we have outlined the expressions for the local Nusselt number below.

Nusselt number The mean temperature can be obtained as $\Theta_m = \int_{-1}^{1} \Theta(\xi,\eta)\bar{u}(\eta)\,d\eta \,/ \int_{-1}^{1} \bar{u}(\eta)d\eta$. Due to a uniform nature of the velocity profile, the mean temperature can be written simply in the form $\Theta_m = \frac{1}{2}\int_{-1}^{1} \Theta(\xi,\eta)\,d\eta$. Therefore, the mean temperature Θ_m have the form

$$\Theta_m = \begin{cases} 1 + \frac{J}{3} + \sum_{n=0}^{\infty} \frac{2\exp(\alpha_n \xi)}{\alpha_n \sqrt{Pe_T^2 \chi^2 + 4\lambda_n^2}} \left(1 + \frac{J}{\lambda_n^2}\right) & ; \text{for isothermal wall} \\ \frac{J + Q_W''}{Pe_T^2 \chi^2}\left(1 + \xi Pe_T \chi\right) & ; \text{for constant heat flux} \end{cases} \tag{20}$$

Using the mean temperature we can write the local Nusselt number in the form $Nu_\xi = h_\xi H / k_f$, where h_ξ is the local heat transfer coefficient and is given by

$$h_\xi = \begin{cases} -\frac{k_f}{H}\left(1 - \Theta_m\right)^{-1} \left.\frac{\partial \Theta}{\partial \eta}\right|_{\eta=1} & ; \text{for Isothermal wall} \\ -\frac{k_f}{H}\left(1 - \Theta_m\right)^{-1} Q_W'' & ; \text{for Constant heat flux} \end{cases} \tag{21}$$

Therefore, the expressions for the local Nusselt number Nu_ξ, for an isothermal condition can be written in the form

$$Nu_\xi = \left\{ J + \sum_{n=0}^{\infty} \frac{2\lambda_n^2 \exp(\alpha_n \xi)}{\alpha_n \sqrt{Pe_T^2 \chi^2 + 4\lambda_n^2}} \left(1 + \frac{J}{\lambda_n^2}\right) \right\} \left\{ \frac{J}{3} + \sum_{n=0}^{\infty} \frac{2\exp(\alpha_n \xi)}{\alpha_n \sqrt{Pe_T^2 \chi^2 + 4\lambda_n^2}} \left(1 + \frac{J}{\lambda_n^2}\right) \right\}^{-1} \tag{22}$$

whereas for constant wall heat flux conditions this can be written as

$$Nu_\xi = Q_W'' \left\{ 1 - \frac{J + Q_W''}{Pe_T^2 \chi^2}\left(1 + \xi Pe_T \chi\right) \right\}^{-1} \tag{23}$$

From the expressions (22) and (23), we can identify the dependence of the viscoelastic behavior of the fluid through the parameter χ.

RESULTS AND DISCUSSIONS

Velocity profile: In typical electroosmotic flows, the values for dimensional parameters for biofluids may be considered as $\rho_f = 10^3 kg/m^3$, $\mu = 10^{-2} - 10^{-1} Pa.s$, $\lambda \approx 10^{-3} - 10^{-1} s$, $\sigma \approx 0.01 - 0.1$, $\varepsilon \approx 10^{-10} C^2/Jm$, $E_x \approx 10^4 - 10^5 V/m$, $\sigma_b \approx 10^{-2} - 10^{-1} S/m$, $\zeta \approx 25 mV$. With these considerations the typical strength of the velocity $U_{HS} \approx 10^{-4} - 10^{-3} m/s$ and characteristic Debye length $\kappa^{-1} \approx 10^{-7} - 10^{-8} m$ (Matias et al. [2015], Xuan et al. [2004b], Curtin et al. [2006], Sun and De Kee [2001]). In this study, we have considered the non-dimensional values according to the reported parametric values in the literature. To adjudicate our simplification as given in equation (10), we depict

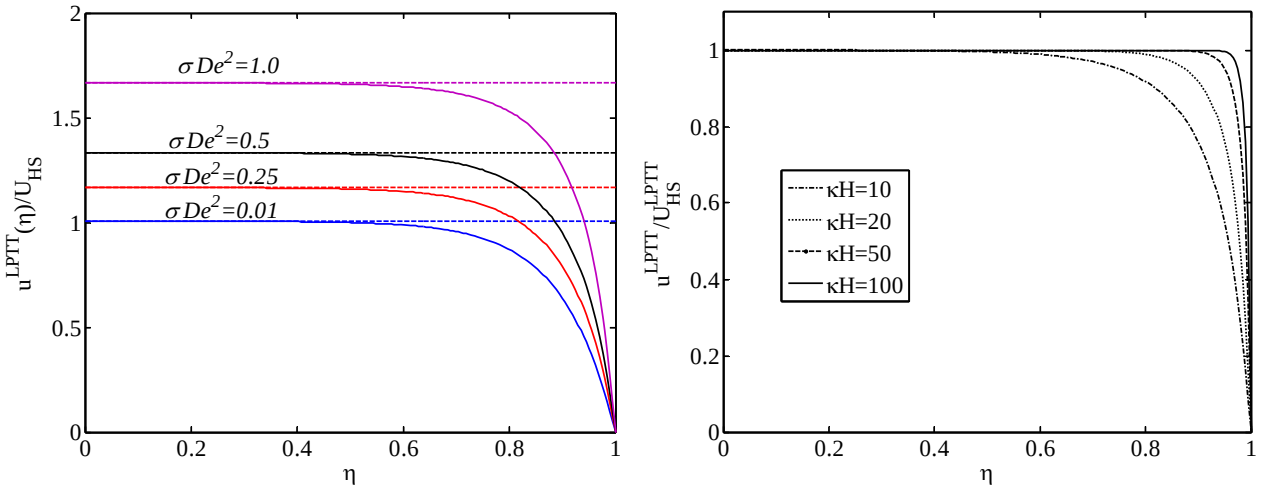

Figure 2: The non-dimensional velocity profile for an electroosmotic flow of linear Phan-Thien-Tanner fluid. (a) Non-dimensionalized with U_{HS} (Helmholtz-Smoluchowski slip velocity for a Newtonian fluid) for different values of the viscoelastic parameter σDe^2. The non-dimensional EDL thickness is considered as $\kappa H = 10$. Dashed lines denotes the HS slip velocity U_{HS}^{LPTT}/U_{HS}. (b) Non-dimensionalized with U_{HS}^{LPTT} for different values of the EDL thickness parameter and $\sigma De^2 = 1$.

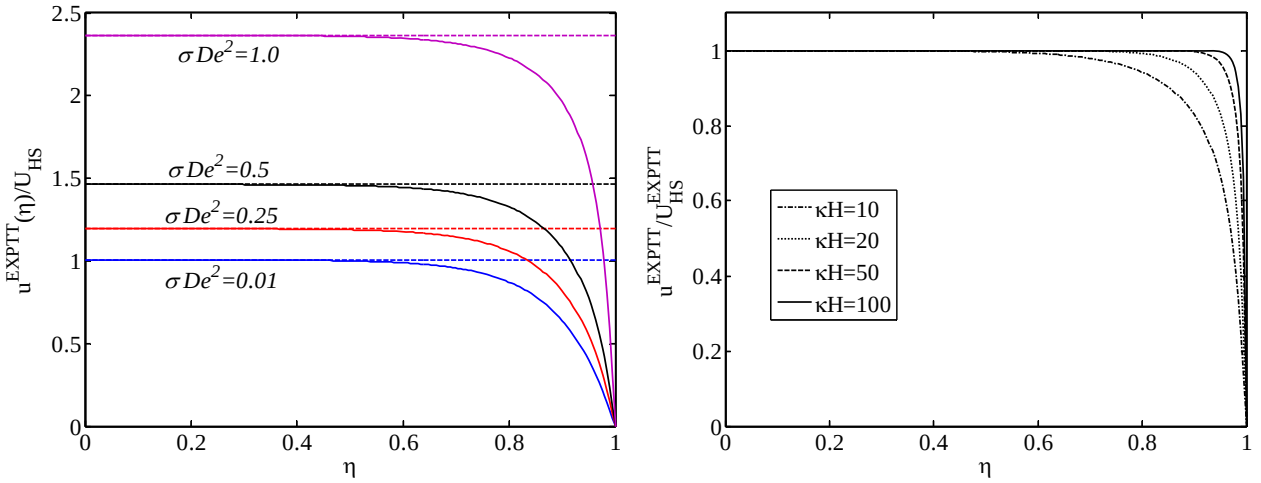

Figure 3: The non-dimensional velocity profile for an electroosmotic flow of exponential Phan-Thien-Tanner fluid. (a) Non-dimensionalized by U_{HS} (Helmholtz-Smoluchowski slip velocity for a Newtonian fluid) for different values of the viscoelastic parameter σDe^2. The non-dimensional EDL thickness is considered as $\kappa H = 10$. Dashed lines denotes the HS slip velocity U_{HS}^{EXPTT}/U_{HS}. (b) Non-dimensionalized with U_{HS}^{EXPTT} for different values of the EDL thickness parameter and $\sigma De^2 = 1$.

the velocity profile from equation (8) (denoted by solid lines) together with equation (10) (denoted by dashed lines) in case of a linear-PTT fluid in Figure 2(a) and exponential-PTT fluid in Figure 3(a), for different values of the viscoelastic parameter σDe^2, where both the velocities are non-dimensionalized by U_{HS}. The increase in σDe^2 is corresponds to the increasing shear thinning behaviour of the fluid, which result in less viscous resistance and hence an increasing velocity is observed from figure 2(a) and 3(a). The velocity is much higher for exponential-PTT fluid compared to the linear-PTT fluid, which is the direct consequence of linearizing the exponential function $Exp\left[\sigma\lambda\tau_{xx}/\mu\right]$. In Figure 2(b) and 3(b), we have plotted the ratios u^{LPTT}/U_{HS}^{LPTT} and u^{EXPTT}/U_{HS}^{EXPTT}, respectively, for

different values of the EDL thickness parameter. As the EDL thickness parameter increases, due to the thinner EDL adjacent to surface, a sharp gradient is observed near the wall and maintains a uniform nature outside the EDL, as seen in typical electroosmotic flows. Therefore, outside the EDL region, the velocity profiles can be approximated as $u^{LPTT} \approx U_{HS}^{LPTT}$ and $u^{EXPTT} \approx U_{HS}^{EXPTT}$. In this study, we have restricted ourselves to the thin EDLs. This consideration may have different advantageous features in studying the thermal characteristics of an EOF of viscoelastic fluid. Because of an almost plug-like velocity profile, the viscous dissipation will have negligible effect (Horiuchi and Dutta [2004]) on the thermal development. Secondly, since the EDL is very thin a larger column of fluid will be exposed nearer the walls and hence will result in more advective thermal transport. Therefore, in the next sub-section we have discussed the thermal characteristics of almost a plug-like EOF of viscoelastic fluids.

Temperature profile In Figure 4(a-b), we have made a comparison between the numerical Laplace inversion and analytical solution of equation (10) for different values of the thermal Peclet' number. Figure 4(a) gives the temperature profile for an isothermal case whereas figure 4(b) represents the case of constant wall heat flux in case of an exponential-PTT fluid. The Joule heat parameter, viscoelastic parameter and the non-dimensional value of the heat flux are considered as $J=1, \sigma De^2=1$ and

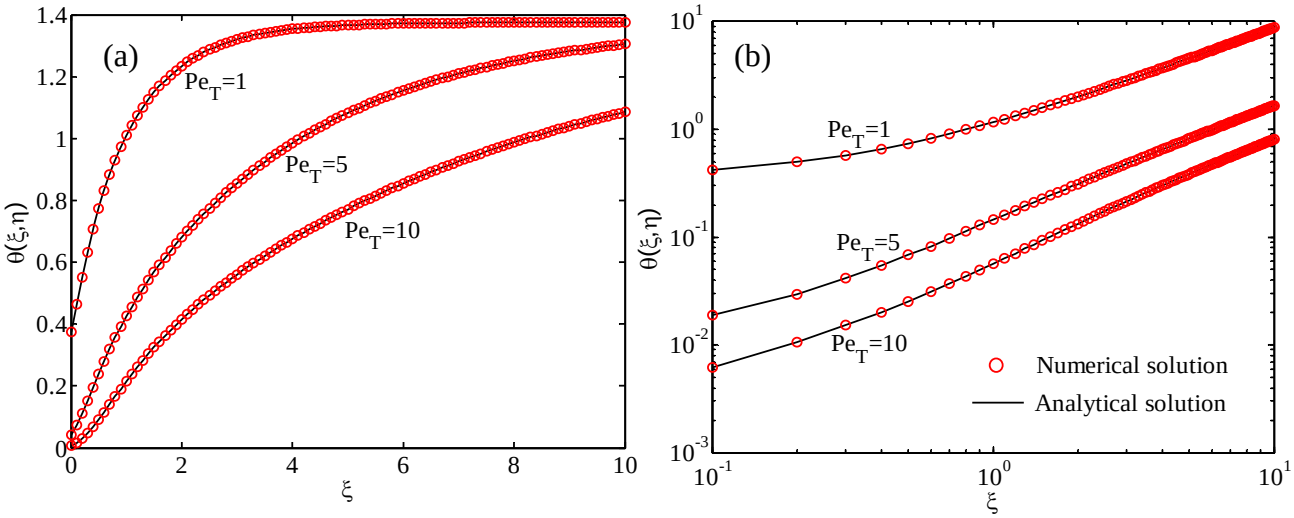

Figure 4: The non-dimensional temperature profile $\Theta(\xi,\eta)$ with respect to the non-dimensional axial co-ordinate ξ at $\eta=0.5$. The other parametric values are $J=1$, $\sigma De^2=1$, $Q_W''=1$. (a) Isothermal wall condition (b) Constant wall heat flux condition.

$Q_W''=1$. In isothermal case the temperature reaches to an asymptotic value, whereas in case of constant heat flux it keeps on increasing. The reason is quite obvious, in isothermal condition the walls are fixed at a temperature together with a specified inlet temperature and Joule heat, which enables the system to reach at an equilibrium point. But, in case of constant heat flux the walls are under continuous heating, which results in increasing fluid temperature. To track this increment, we have plotted the difference between the wall temperature and the temperature at different heights of the microchannel, that is the quantity $\Theta(\xi,1)-\Theta(\xi,\eta)$ with respect to η, in Figure 5(a) at different axial location ξ and $Pe_T=1$. As the flow progresses, the difference reaches to a maximum value of 0.5 at a distance $\xi=10$ from the channel entrance. To identify the effect of the viscoelastic parameter on the temperature difference, we fix up the axial location at $\xi=1$ and plotted the quantity $\Theta(\xi,1)-\Theta(\xi,\eta)$ with respect to η, in Figure 5(b) for different values of σDe^2. For small values of σDe^2, the difference almost reaches the value 0.5, but with increasing σDe^2 the

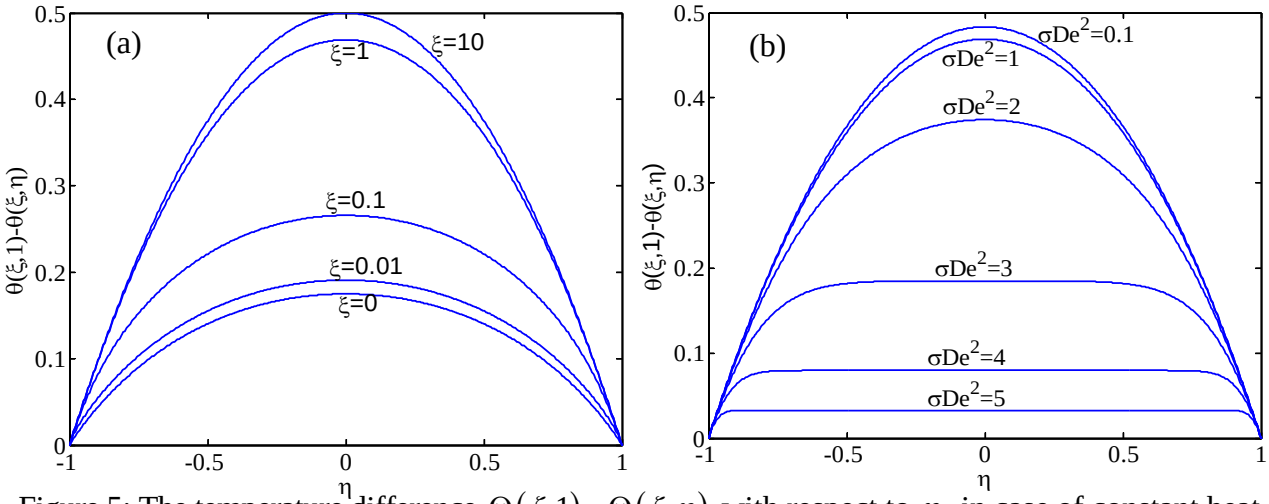

Figure 5: The temperature difference $\Theta(\xi,1)-\Theta(\xi,\eta)$ with respect to η in case of constant heat flux condition and exponential-PTT fluid. (a) At different axial location for $\sigma De^2=1$(b) For different values of the viscoelastic parameter σDe^2 at the location $\xi=1$. The other parametric values are $Q_W''=1$, $J=1$ and $Pe_T=1$.

difference decreases. The increase in σDe^2 eventually increases the fluid velocity by virtue of the shear-thinning behaviour of the fluid, which in turn increases the advective heat transfer by the fluid. At the specified location , $\xi=1$, the temperature does not reaches to its fully developed state and hence require a larger length to reach the value 0.5. A similar behaviour is also seen in case of a linear-PTT fluid.

In Figure 6(a) we present a comparison for the temperature distribution between a linear-PTT fluid and an exponential-PTT fluid in case of isothermal walls. The heat transfer due to an exponential-PTT fluid within the microchannel is larger compared to the linear-PTT fluid. For small thermal Peclet number Pe_T the centreline temperature reaches to a maximum value from the wall temperature $\Theta(\xi,1)=1$. As the value of Pe_T increases, the maximum value decreases. A small Pe_T corresponds to the lower advective heat transport due to the fluid flow, so this increment is from the Joule heat

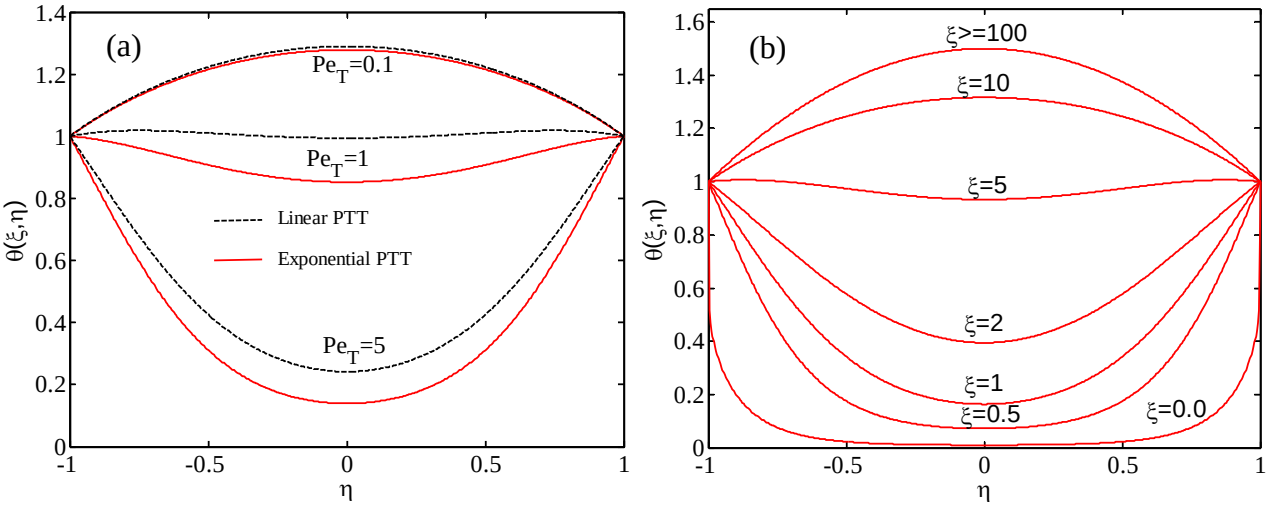

Figure 6: (a) A comparison in the temperature distribution for a linear-PTT and an exponential-PTT fluid with isothermal wall condition and at $\xi=1$. (b) The temperature distribution for an exponential-PTT fluid at different axial position and $Pe_T=10$. The other parametric values are $\sigma De^2=0.1$ and $J=1$.

and wall temperature. In case of larger Pe_T number, there is a significant contribution from the advective transport which balances out the heat rise due to Joule heat and wall temperature and hence a decrease in the centreline temperature. When looked into (Figure 6(b)) the temperature at different entrance length ξ of the channel, initially the temperature decreases from its wall temperature $\Theta(\xi,1)=1$ to a minimum value. The case considered in Figure 6(b) is for $Pe_T=10$. At small values of ξ, the fluid does not get enough length to develop the heat within the system via the advective transport. But as ξ increases, the temperature reaches to a maximum value. In this case, the temperature reaches to the value 1.5 at all values of ξ greater than 100. A similar behaviour can also be seen for variation in the viscoelastic parameter. In Figure 7(a-b), we have shown the

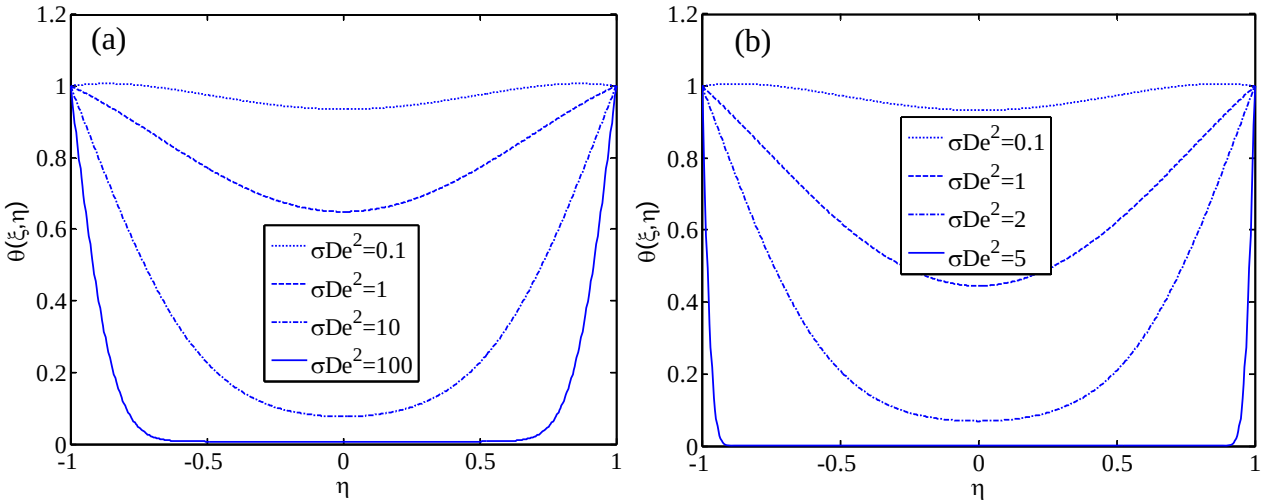

Figure 7: The temperature distribution for viscoelastic fluids at different value of σDe^2 with isothermal wall condition. (a) A linear-PTT fluid and (b) An exponential-PTT fluid. The other parametric values are $Pe_T=10$, $\xi=5$ and $J=1$.

temperature distribution for linear-PTT and exponential-PTT fluid at different values of the viscoelastic parameter at an axial location $\xi=5$ and $Pe_T=10$. In case of a linear-PTT fluid (Figure 7(a)), the increase in σDe^2, increases the advective transport of heat by virtue of an increasing plug velocity of the fluid. This increment is much larger for an exponential-PTT fluid (Figure 7(b)) compared to linear-PTT fluid. Because of the higher plug velocity, the advective transport is become dominant over Joule heat and the fluid temperature decreases sharply from its maximum value 1 to 0 at the central line, which is the non-dimensional inlet temperature.

CONCLUSIONS

In this study, we have obtained an analytical solution for the heat transfer coefficient in electroosmotically driven viscoelastic flow (linear-PTT fluid and exponential-PTT fluid) in parallel plate microchannel. First, we have derived an analytical solution for the EOF of viscoelastic fluid and approximated by a Helmholtz-Smoluchowski type slip velocity. Using this HS-slip velocity, we have reduced the energy equation and solved it by Laplace transform method. Two types of boundary condition is used, isothermal wall and constant wall heat flux. In inverting the expressions for temperature, we employed residue calculus to obtain the analytical solution and a Fourier series based method for the numerical solution. The analytical solution for the temperature profile exactly matches with the numerical solution. We have also obtained the analytical expression for the local Nusselt number for both isothermal and constant wall heat flux conditions. The increase in viscoelastic parameter increases the plug velocity which in turn increases the net advective heat transfer within the microchannel. This advective transport is larger for exponential-PTT fluids compared to linear-PTT fluids.

Acknowledgemets The author PG gratefully acknowledges the financial support and International Travel Support from Science and Engineering Research Board, Department of Science and Technology, India, through the project YSS/2015/000729 and ITS/530/2017-18.

REFERENCES

Bautista, O., Sanchez, S., Arcos, J.C., and Mendez, F., 2013, "Lubrication Theory for Electro-osmotic Flow in a Slit Microchannel with the Phan-Thien and Tanner Model", *J. Fluid Mech*., 722, pp. 496-532.

Broderick, S. L., Webb, B. W., and Maynes, D., 2005, "Thermally Developing Electro-osmotic Convection in Microchannels with Finite Debye-Layer Thickness", *Numerical Heat Transfer, Part A*, 48, pp. 941–964.

Chen, C. H., 2009, "Thermal Transport Characteristics of Mixed Pressure and Electro-Osmotically Driven Flow in Micro- and Nanochannels With Joule Heating," *ASME J. Heat Transfer*, 131, p. 022401.

Coelho, P. M., Alves, M. A. and Pinho, F. T., 2012, "Forced convection in electroosmotic/poiseuille micro-channel flows of viscoelastic fluids: fully developed flow with imposed wall heat flux". *Microfluid Nanofluid*, 12, pp. 431–449.

Curtin, D. M., Newport, D. T., and Davies M. R., 2006, "Utilising m-PIV and pressure measurements to determine the viscosity of a DNA solution in a microchannel," *Exp. Therm. Fluid Sci*., 30, pp. 8433-8852.

Das, S., and Chakraborty, S., 2006, "Analytical Solutions for Velocity, Temperature and Concentration Distribution in Electroosmotic Microchannel Flows of a Non-Newtonian Bio-Fluid," *Anal. Chim. Acta*, 559, pp. 15–24.

Dey, R., Chakraborty, D., and Chakraborty, S., 2011, "Analytical Solution for Thermally Fully Developed Combined Electroosmotic and Pressure-Driven Flows in Narrow Confinements with Thick Electrical Double Layers," *ASME J. Heat Transfer*, 133, p. 024503.

Dey, R., Ghonge, T., and Chakraborty, S., 2013, "Steric-Effect-Induced Alteration of Thermal Transport Phenomenon for Mixed Electroosmotic and Pressure Driven Flows Through Narrow Confinements," *Int. J. Heat Mass Transfer*, 56(1–2), pp. 251–262.

Dutta, P., Horiuchi, K., and Yin, H.-M., 2006, "Thermal Characteristics of Mixed Electroosmotic and Pressure-Driven Microflows," *Comput. Math. Appl.*, 52(5), pp. 651–670.

Escandon, J. P., Bautista, O., and Mendez, F., 2013, "Entropy Generation in Purely Electroosmotic Flows of Non-Newtonian Fluids in a Microchannel," *Energy*, 55, pp. 486–496.

Escandon, J. P., Bautista, O., Mendez, F., and Bautista, E., 2011, "Theoretical Conjugate Heat Transfer Analysis in a Parallel Flat Plate Microchannel under Electro-Osmotic and Pressure Forces With a Phan-Thien-Tanner Fluid," *Int. J. Therm. Sci.*, 50(6), pp. 1022–1030.

Iverson, B.D., Maynes, D., and Webb, B. W., 2004, "Thermally Developing Electroosmotic Convection in Rectangular Microchannels with Vanishing Debye-Layer Thickness", *J. Thermophysics Heat Transfer*, 18, pp. 486-493.

Goswami, P., Mondal, P. K., Dutta, A. and Chakraborty, S., 2016, "Entropy Generation Minimization in an Electroosmotic Flow of non-Newtonian Fluid: Effect of Conjugate Heat Transfer," *ASME J. Heat Transfer*, 138, p. 051704.

Horiuchi, K., and Dutta, P., 2004, "Joule Heating Effects in Electroosmotically Driven microchannel Flows," *Int. J. Heat Mass Transfer*, 47(14–16), pp. 3085–3095.

Hunter, R. J., 1981, *Zeta Potential in Colloid Science: Principles and Applications*, Academic Press, New York.

Matias, A., Sanchez, S., Mendes, F., and Bautista, O., 2015, "Influence of slip wall effect on a non-isothermal electro-osmotic flow of a viscoelastic fluid," *Int. J. Thermal Sci.*, 98, pp. 352-363.

Maynes, D., and Webb, B. W., 2003a, "Fully-Developed Thermal Transport in Combined Pressure and Electro-Osmotically Driven Flow in Microchannels," *J. Heat Transfer*, 125, pp. 889–895.

Maynes, D., and Webb, B. W., 2003b, "Fully Developed Electroosmotic Heat Transfer in Microchannels," Int. J. Heat Mass Transfer, 46, pp. 1359–1369.

Maynes, D., and Webb, B. W., 2004, "The Effect of Viscous Dissipation in Thermally Fully-Developed Electro-Osmotic Heat Transfer in Microchannels," *Int. J. Heat Mass Transfer*, 47(5), pp. 987–999.

Park, H. M., and Lee, W. M., 2008a, "Helmholtz–Smoluchowski velocity for viscoelastic electroosmotic flow," *J. Colloid Interface Sci.*, 317, pp. 631-636.

Park, H. M., and Lee, W. M., 2008b,"Effect of viscoelasticity on the flow pattern and the volumetric flow rate in electroosmotic flows through a microchannel," *Lab Chip*,8, pp. 1163-1170.

Probstein, R. F., 1994, *Physiochemical Hydrodynamics: An Introduction*, Wiley, New York.

Rice, R. G. and Do, D. D., 1995, *Applied Mathematics and Modeling for Chemical Engineers*, Wiley, New York.

Sadeghi, A., and Saidi, M.H., 2010, "Viscous Dissipation Effects on Thermal Transport Characteristics of Combined Pressure and Electroosmotically Driven Flow in Microchannels," *Int. J. Heat Mass Transfer*, 53, pp. 3782–3791.

Sadeghi, A., Saidi, M.H., and Mozafari, A. A., 2011, "Heat Transfer due to Electroosmotic Flow of Viscoelastic Fluids in a Slit Microchannel". *Intl J. Heat Mass Transfer*, 54, pp. 4069–4077.

Sanchez, S., Arcos, J., Bautista, O., and Mendez, F., 2013, "Joule Heating Effect on a Purely Electroosmotic Flow of Non-Newtonian Fluids in a Slit Microchannel," *J. Non-Newtonian Fluid Mech.*, 192, pp. 1–9.

Sun, N. and De Kee, D., 2001, "Simple shear, hysteresis and yield stress in biofluids," *Can. J. Chem. Eng.*, 79, pp. 843-852.

Tang, G. Y., Yang, C., Chai, J. C., and Gong, H. Q., 2004, "Joule Heating Effect on Electroosmotic Flow and Mass Species Transport in a Microcapillary," *Int. J. Heat Mass Transfer*, 47(2), pp. 215–227.

Xuan, X., 2008, "Joule heating in electrokinetic flow". *Electrophoresis*, 29, pp. 33–43.

Xuan, X. and Li, D., 2005, "Analytical study of Joule heating effects on electrokinetic transportation in capillary electrophoresis." *J. Chromatogr. A*, 1064, pp. 227–237.

Xuan, X., Sinton, D. and Li, D., 2004a, "Thermal end effects on electroosmotic flow in a capillary." *Intl J. Heat Mass Transfer*, 47, pp. 3145–3157.

Xuan, X., Sinton, D. and Li, D., 2004b, "Electroosmotic flow with joule heating effects." *Lab on a Chip*, 4, pp. 230–236.

Yavari, H., Sadeghi, A., Hassan Saidi, M., and Chakraborty, S., 2013,"Temperature Rise in Electroosmotic Flow of Typical Non-Newtonian Biofluids Through Rectangular Microchannels," *ASME J. Heat Transfer*, 136(3), p. 031702.

Zhao, C. and Yang, C., 2013, "Electrokinetics of non-Newtonian fluids: A review". Adv. Colloid Interface Sci., 201-202, pp. 94-108.